GENE POLYMORPHISMS OF THE RECEPTOR FOR ADVANCED GLYCATION END PRODUCTS AND ITS ROLE IN THE AGE-RAGE PATHWAY AND INFLAMMATION

by

Gladys Shaw

A Thesis
Submitted to the
Graduate Faculty
of
George Mason University
in Partial Fulfillment of
The Requirements for the Degree
of
Master of Science
Biology

Committee:

_____	Dr. Ancha Baranova, Committee Chair
_____	Dr. Aybike Birerdinc, Thesis Director
_____	Dr. Karl Fryxell, Committee Member
_____	Dr. Iosif Vaisman, Acting Director, School of Systems Biology
_____	Dr. Donna Fox, Associate Dean, Office of Student Affairs & Special Programs, College of Science
_____	Dr. Peggy Agouris, Dean, College of Science

Date: _____ Summer Semester 2017
George Mason University
Fairfax, VA

Gene Polymorphisms of the Receptor for Advanced Glycation End Products and Its Role in the AGE-RAGE Pathway and Inflammation

A Thesis submitted in partial fulfillment of the requirements for the degree of Master of Science at George Mason University

by

Gladys Shaw
Bachelor of Science
The College of William and Mary, 2015

Thesis Director: Dr. Aybike Birerdinc, Research Assistant Professor
School of Systems Biology

Summer Semester 2017
George Mason University
Fairfax, VA

ACKNOWLEDGEMENTS

First and foremost, I would like to thank Dr. Aybike Birerdinc and Dr. Ancha Baranova for allowing me to conduct research for this project. I would also like to thank Dr. Rohini Mehta for introducing me to the topic and clarifying any concerns that come up. Additionally, I would like to thank the student members of the lab, the School of Systems Biology at George Mason University, and the Betty and Guy Beatty Center for Integrated Research of Inova Health Systems for their resources.

TABLE OF CONTENTS

LIST OF TABLES

LIST OF FIGURES

LIST OF ABBREVIATIONS AND SYMBOLS

A Disintegrin and metalloproteinase domain-containing protein 10 ..... ADAM10
Activator protein 1 ..... AP-1
Advanced glycation end product ..... AGE
Advanced glycation end product receptor (gene) ..... *AGER*
Alanine Aminotransferase ..... ALT
Aspartate Aminotransferase ..... AST
Base pair ..... bp
Beta amyloid ..... aβ
Body mass index ..... BMI
Bovine serum albumin ..... BSA
Carboxymethylysine ..... CML
Cardiovascular disease ..... CVD
Computed tomography ..... CT
Concentration ..... Conc
Degrees Celsius ..... ºC
Degrees of freedom ..... D.F.
Deoxyribonucleic acid ..... DNA
Diaphanous-related formin 1 ..... Dia-1
Diethyl pyrocarbonate ..... DEPC
Dominant negative receptor for advanced glycation end products ..... DN-RAGE
Endogenous secretory receptor for advanced glycation end products ..... esRAGE
Enzyme-linked immunosorbent assay ..... ELISA
Expiration date ..... Exp
Extreme groups approach ..... EGA
Endoglucanase 1 ..... END-1
Glyoxal-lysine dimer ..... GOLD
Gravity ..... g
Greater than or equal to ..... ≥
Greater than ..... >
Health Insurance Portability and Accountability Act of 1996 ..... HIPAA
High mobility group protein B1 ..... HMGB1
High-density lipoprotein ..... HDL
Horseradish peroxidase ..... HRP
Human immunodeficiency virus ..... HIV
Interleikin-1 ..... IL-1
Interleikin-6 ..... IL-6

Interleikin-8 ..... IL-8
Interquartile range ..... IQR
Janus kinase ..... JAK
Kilobase ..... kb
Kilogram ..... kg
Less than or equal to ..... ≤
Less than ..... <
Lot number ..... Lot
Low-density lipoprotein ..... LDL
Magnetic resonance imaging ..... MRI
Mallory-Denk body ..... MALLORY_BIN
Matrix metallopeptidase-9 ..... MMP-9
Messenger Ribonucleic acid ..... mRNA
Meter ..... m
Microliter ..... μL
Mild abnormal ..... Mild Ab
Milligram ..... mg
Milliliter ..... mL
Minute ..... min
Mitogen-activated protein kinase ..... MAPK
Monocyte chemoattractant protein-1 ..... MCP-1
Nanometer ..... nm
Nicotinamide adenine dinucleotide ..... NADH
No disease ..... No dis
Non-alcoholic fatty liver disease ..... NAFLD
Non-alcoholic fatty liver ..... NAFL
Non-alcoholic steatohepatitis ..... NASH
Non-template control ..... NTC
N-truncated receptor for advanced end products ..... NT-RAGE
Nuclear factor kappa-light-chain-enhancer of activated B cells ..... NF-κB
Phosphate-buffered saline ..... PBS
Phosphoinositide 3-kinase PI3K
Phospholipase C ..... PLC
Pictogram ..... pg
Plus or minus ..... ±
Polymerase chain reaction ..... PCR
Potential of hydrogen ..... pH
Product number ..... PN
Protein kinase C ..... PKC
Quantative polymerase chain reaction ..... qPCR
Receptor for Advanced Glycation End Products (protein) ..... RAGE
Ribonucleic acid ..... RNA
Rotations per minute ..... RPM
Second ..... s

Signal transducers and activators of transcription ..... STAT
Single nucleotide polymorphism ..... SNP
Soluble (cytosolic) receptor for advanced glycation end products ..... sRAGE
Standard deviation ..... SD
Tissue factor ..... TF
Total cholesterol ..... TCHOL
Triglyceride ..... TRIG
Tumor necrosis factor alpha ..... TNF-α
Type 2 Diabetes T2D
Ultraviolet ..... UV
United States of America ..... USA
Vascular cell adhesion protein 1 ..... VCAM-1
Visceral adipose tissue ..... VAT
White blood cell ..... WB

ABSTRACT

GENE POLYMORPHISMS OF THE RECEPTOR FOR ADVANCED GLYCATION END PRODUCTS AND ITS ROLE IN THE AGE-RAGE PATHWAY AND INFLAMMATION

Gladys Shaw, M.S.

George Mason University, 2017

Thesis Director: Dr. Aybike Birerdinc

Advanced glycation end products (AGEs) are cross-linked, non-degradable aggregates of proteins, lipids and nucleic acids produced during aging and many aging-associated chronic diseases. Additionally, the receptor for advanced glycation end products (RAGE) is an important receptor in the pro-inflammatory pathway. Clinically, metabolic diseases associated with inflammation, such as diabetes, non-alcoholic fatty liver disease (NAFLD), and obesity, may be exacerbated by a) Varying levels of RAGE isoforms; b) Polymorphisms in *AGER*, the gene encoding RAGE, may influence ligand-receptor interaction or RAGE levels; c) Variations in concentration of RAGE's ligand, advanced glycation end products (AGE). These variations will alter inflammatory milieu within the human body. TaqMan qPCR was employed in genotyping of 4 inflammation-related SNPs located within the *AGER* gene (T-429C, T-374A, Gly82Ser/G344A, and G1704T) in 340 obese patients. ELISA assays were used in the analysis of RAGE protein isoforms in the serum of these patients. Statistic-based haplotype and individual genotype analysis

was used to determine whether a particular genotype/haplotype of the *AGER* locus produces significantly different levels of RAGE protein in those with varying levels of non-alcoholic fatty liver disease. Correlations between liver histopathology and frequencies of specific *AGER* haplotypes, T-429 – A-374 – Gly82/G344 – G1704 and T-429 – A-374 – Gly82/G344 – T1704 were detected. Additionally, a significant difference between AGE levels in patient sera were discovered between the "mild abnormality of liver parenchyma" and the "no disease" group, yet this significance was not maintained when patients were separated based upon their diabetes status. This work can be used as a foundation for future studies aiming to untangle the complex nature of AGE-RAGE interactions and inflammation in morbidly obese populations.

INTRODUCTION

As body weight increases amongst the general population, so do the diseases that come with the accumulation of visceral adipose tissue (VAT). Likewise, there has been a consistent increase in the prevalence of non-alcoholic fatty liver disease (NAFLD), the most common liver condition in America, with approximately a quarter (25%) of the population having a fatty liver (Gitto et al., 2016; Neuschwander-Tetri, 2017; Townsend and Newsome, 2016; Yki-Järvinen, 2016). NAFLD is a spectrum of diseases that range from steatosis, known simply as non-alcoholic fatty liver (NAFL), to non-alcoholic steatohepatitis (NASH) (Younossi et al., 2014). Although 45%-100% of those with NAFLD are asymptomatic, those who do show symptoms report confusion, nausea, fatigue, jaundice, and pain in the upper right quadrant of the abdominal region (Mehta and Younossi, 2012; Younossi et al., 2014).

Clinical diagnosis of fatty liver

Diagnosis of NAFLD can be established by non-invasive imaging modalities, including ultrasound, magnetic resonance imaging (MRI), and computed tomography (CT), or by the detection of liver steatosis and/or fibrosis in absence of other factors commonly known to provoke chronic liver disease, i.e. alcohol abuse or viral infections (Baršić et al., 2012; Mehta and Younossi, 2012; Neuschwander-Tetri, 2017; Yki-Järvinen, 2016). In approximately 2% - 5% of all NAFLD cases, and in 30% - 40% of

those with both NAFLD and type 2 diabetes (T2D), the disease eventually progresses to NASH (Cusi, 2016; Mehta and Younossi, 2012; Neuschwander-Tetri, 2017). NASH, defined as "steatosis as well as presence of inflammation and hepatocellular ballooning or other evidence of hepatocyte injury" (Younossi et al., 2014), is diagnosed via liver biopsy, which is the gold standard technique for the assessment of liver health. Due to the invasive nature of this assessment, non-invasive methods are urgently needed to assure early detection, limit progression to cirrhosis, and increase survival. Currently, there is no pharmaceutical cure for NAFLD, yet it can be mitigated through lifestyle changes, including diet and exercise (Henao-Mejia et al., 2012).

RAGE receptor and its functions

The receptor for advanced glycation end products (RAGE) is a protein of immunoglobulin superfamily, and is ubiquitously expressed at low levels in human tissues, except the lungs, in which it is found in comparatively higher levels than in other body areas (Sparvero et al., 2009). RAGE has been implicated in many systemic inflammation-driven disorders, such as type 2 diabetes (Oliveira et al., 2013), cardiovascular diseases (CVD) (Kalousová et al., 2007; Peng et al., 2013) and renal dysfunction (Tomino et al., 2011).

RAGE Interactions with AGE

When bound to one of its ligands, advanced glycation end products (AGE), the membrane bound RAGE receptor triggers a pathway commonly activated in chronic inflammatory phenotypes. AGEs are cross-linked, non-degradable macromolecules that

are generated during carbonyl stress. Specifically, AGEs are proteins and lipids glycated through the Mallard reaction, a non-enzymatic biochemical reaction with extracellular reducing sugars (Matsumoto et al., 2008; Uribarri et al., 2010).

As shown in Figure 1, the Mallard reaction takes a considerable amount of time to occur. After the reaction begins, a Schiff base is formed, which at this point is reversible. Next, this transforms into an Amadori product, which is a stable intermediate between the Schiff stage and the mature AGE. This modified product then undergoes a long transition into a mature AGE through repetitions of oxidation, dehydration, and condensation reactions (Oliveira et al., 2013). Because of the increased levels of blood glucose in diabetic individuals, there is an increased chance of AGE product formation. AGEs may also be introduced exogenously via diet, as broiling or grilling/charring foods increases AGE intake in high fat, high calorie (i.e. typical "Western") foods, yet the mechanism of its gastric absorption is unclear (Goldberg et al., 2004; Uribarri et al., 2005). Moreover, Uribarri et al. reported that an increase of the consumption of AGE rich foods in diabetic patients is paralleled by activation of RAGE-mediated pathways, including those that lead to NF-κB and VCAM-1 expression, and MAPK phosphorylation in human endothelial cell cultures (Uribarri et al., 2005). In a 2016 study by Leung et al., high fat and high calorie foods enriched by AGEs due to their preparation, i.e. frying, broiling, or grilling, were shown to exacerbate the levels of inflammation in murine NASH models via the RAGE pathway (Leung et al., 2016). Additionally, it was noted that patients with known liver disease have difficulties clearing out accumulated AGEs from their blood, as the liver is pivotal in this process (Su et al., 2015).

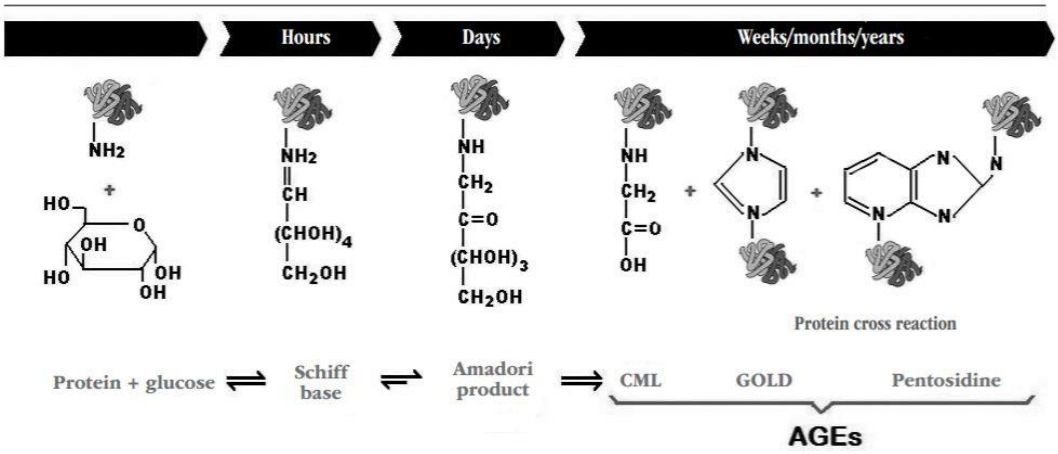

Figure 1 : The formation of advanced glycation end products (AGEs) via the Mallard reaction. This process may cycle for months to years, creating AGEs in the body. CML=carboxymethyllysine. GOLD = glyoxal-lysine dimer. Adopted from Oliveira et al, 2013.

Clinical courses of inflammatory metabolic diseases, such as type 2 diabetes, NAFLD, and NASH, may be intensified by an increase in AGE-RAGE interactions (Takeuchi et al., 2015). The AGE-RAGE pathway triggers multiple secondary pathways (Figure 2), including PKC, PI3K, and MAPK, which collectively activate the transcription factors AP-1 and NF-κB (Piperi et al., 2015). These transcription factors increase the secretion of well-known pro-inflammatory cytokines within hepatocytes, such as IL-1, IL-6, IL-8 and TNFα, and create a positive feedback loop by enhancing expression of RAGE on cellular membranes. As a result, fatty liver condition is exacerbated (Henao-Mejia et al., 2012; Mehta et al., 2013; Oliveira et al., 2013). Since some instances of NAFLD can progress to permanent damage such as cirrhosis, early detection is critical.

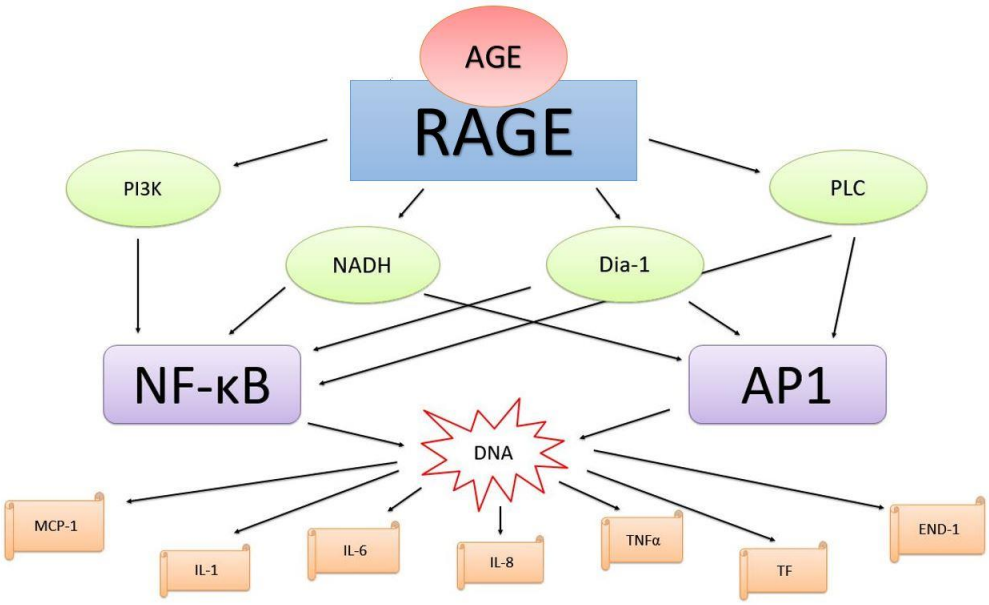

Figure 2 : Simplified schematic of the inflammatory signaling pathway of the AGE-RAGE interactions. As AGE binds to its receptor, RAGE, PI3K, NADH, Dia-1, and PLC are released in the cell's cytoplasm. This, in turn, activates the transcription factors, NF-κB and AP1, which then enter the nucleus and increase the transcription of the pro-inflammatory cytokines MCP-1, IL-1, IL-6, IL-8, TNF-α, TF, and END-1. Additionally, the AGE-RAGE interaction forms a positive feedback loop, increasing the amount of RAGE transcribed and expressed (not shown).

Other ligands of RAGE

In addition to AGEs, RAGE binds to β-amyloid peptide and S100 calgranulin, as well as some other ligands, all of which bind to the V-type domain of the receptor (Figure 3). The two C-type domains bind to β amyloid, S100A12 (C1, Figure 3), and S100A6 (C2, Figure 3). These ligands all play a role in inflammation (Figure 2), and must be considered in studies accessing the activation of RAGE receptors (Lorenzi et al., 2014).

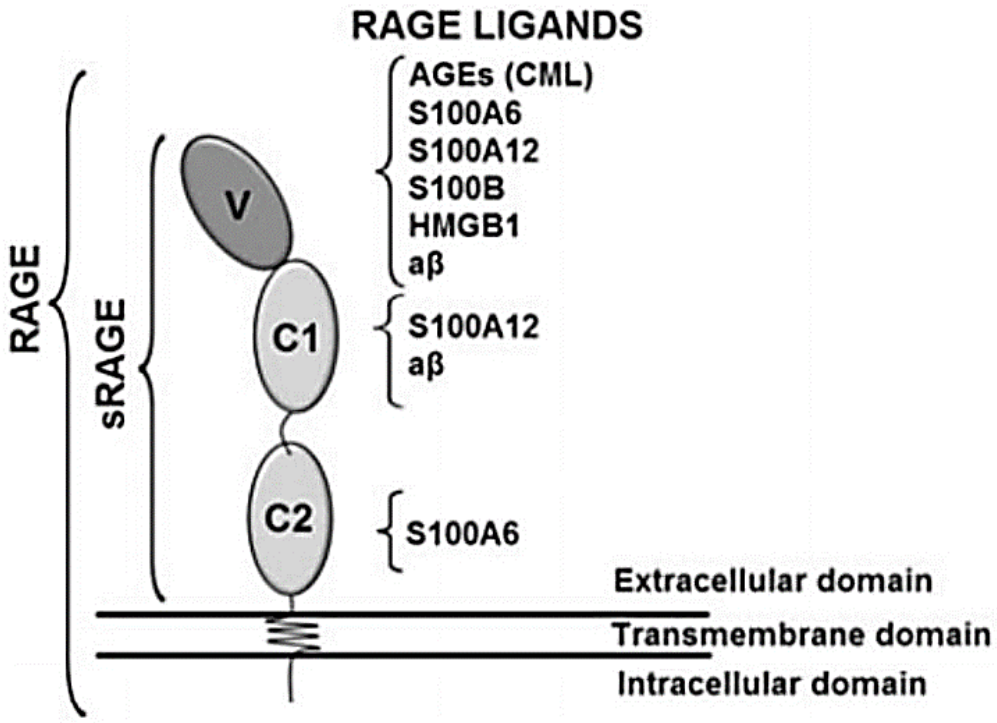

Figure 3 : Main ligands for RAGE, including AGE. All the ligands bind to the V-type domain, with additional binding sites for β amyloid (aβ) and S100A12 on the C-type domain closest to the N-terminal, and an additional binding site for S100A6 on the C-type domain closest to the cell membrane. Adopted from Lozenzi et al., 2014.

Isoforms of RAGE

In humans, the RAGE protein is found in four main forms (

Figure 4). Cytosolic or soluble RAGE (sRAGE), also known as endogenous secretory RAGE (esRAGE), and membrane bound RAGE (RAGE) are two isoforms most commonly explored in the literature (Vazzana et al., 2009). The other two isoforms are its truncated versions, namely, the dominant negative version of the receptor (DN-RAGE), which lacks a cytosolic tail, and the N-truncated form (NT-RAGE), which lacks the V-region of the N-terminal. Both DN-RAGE and NT-RAGE are encoded by naturally

occurring mRNA splice variants, and are less commonly studied (Ding and Keller, 2005; Tan et al., 2007).

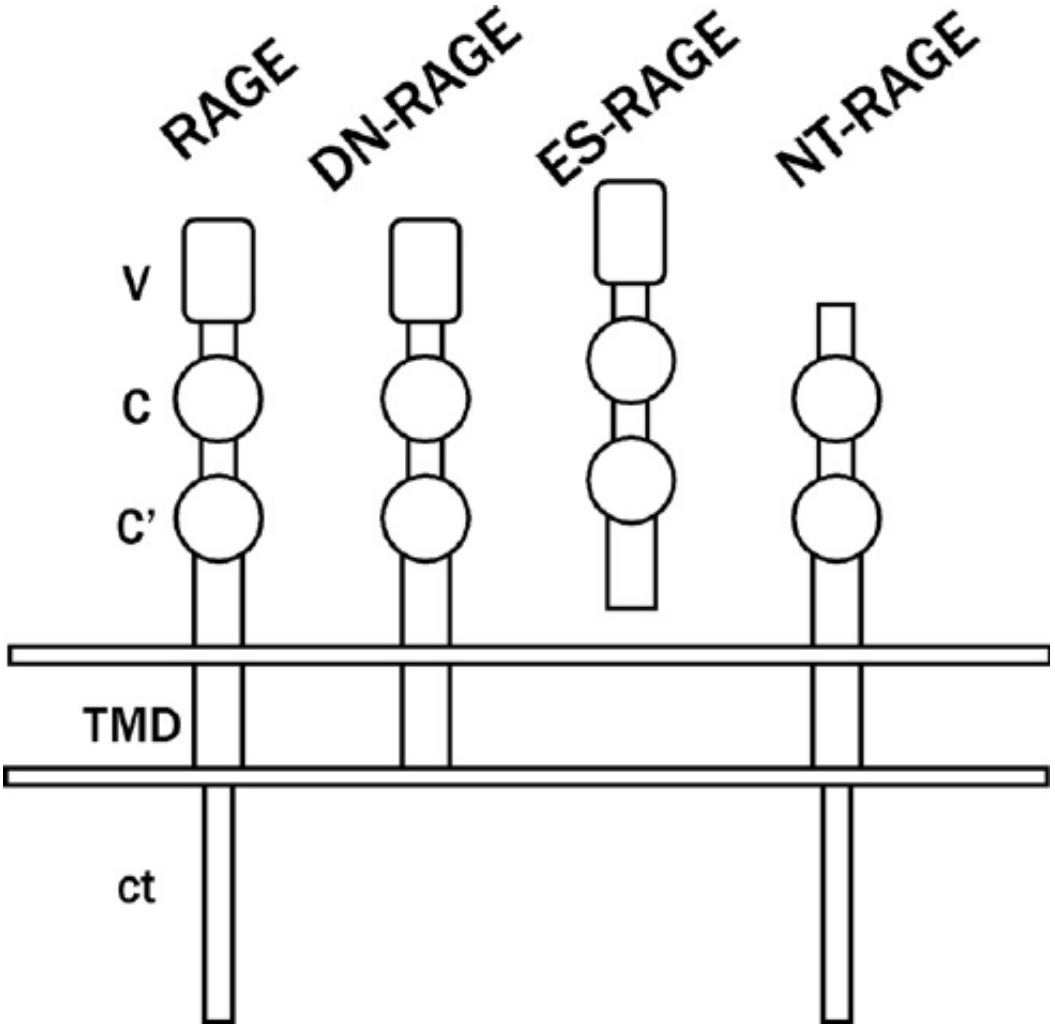

Figure 4 : Most common isoforms of RAGE. The most common, full length isoform of RAGE includes an N-terminal with one V-type domain, lying closest to the amino terminal, and two C-type domains which lay extracellularly, a transmembrane domain, and a cytosolic tail. Dominant negative RAGE lacks a cytosolic tail on the carboxyl end. esRAGE, or soluble RAGE, lacks both the transmembrane domain and cytosolic tail. Lastly, N-truncated RAGE lacks the V-type domain in its N-terminal. These variants arise via alternative splicing of the RAGE mRNA. Figure adopted from Tan et al., 2007.

Cytosolic cleavage of RAGE

The most common product of the advanced glycosylation end product specific receptor, the gene that encodes the RAGE protein (*AGER),* is full length RAGE, a transmembrane receptor with a cytosolic tail. Regarding soluble sRAGE, there are two similar yet distinct isoforms, distinguished by their formation *in vivo* (

Figure 5). EsRAGE, one of the circulating forms of RAGE (sRAGE), is produced via alternative splicing of *AGER*. Thus, esRAGE has no transmembrane or cytosolic domains and is destined to be soluble from the start (Vazzana et al., 2009) (

Figure 5). Despite this, the presence of fully formed V and C domains allows the variant to bind to ligands without transmitting signals that trigger inflammatory sequelae. Consequently, esRAGE is considered to protect against the signaling triggered by AGEs, as it acts as a key inhibitor of carbonyl stress response due to its inability to signal downstream when bound to ligand.

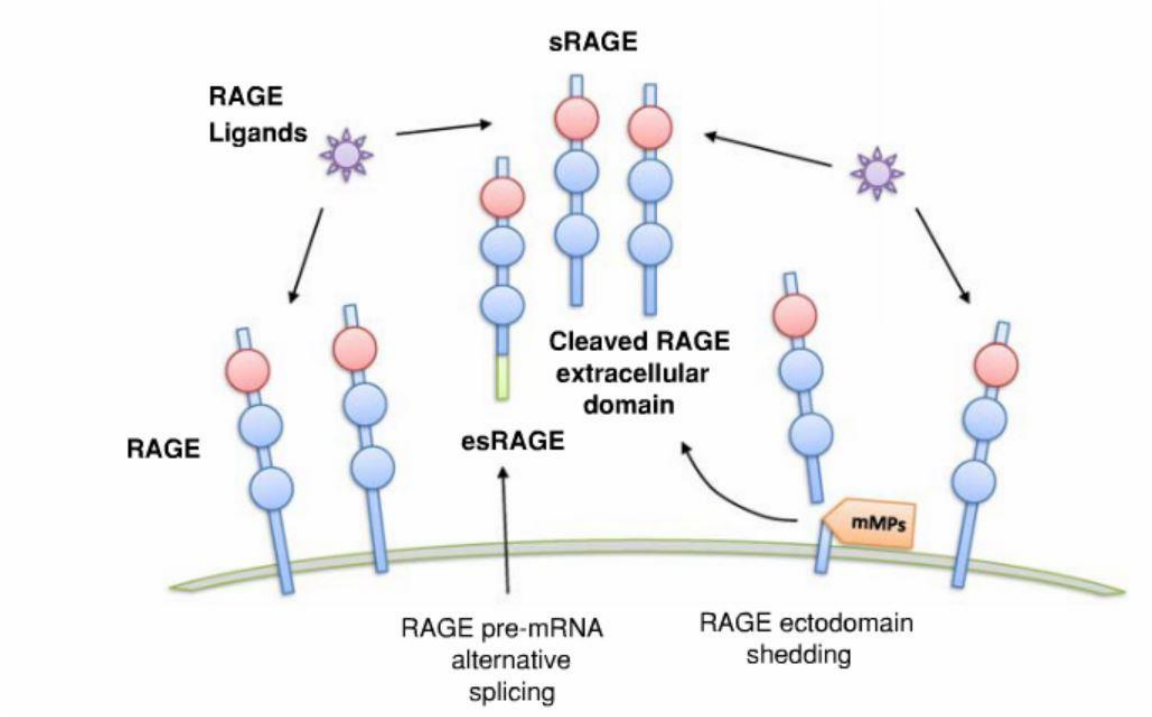

Figure 5 : sRAGE may be made with the aid of two mechanisms. The first is through splicing of full length RAGE mRNA to create sRAGE via translation of this sequence. The second is through shedding of the extracellular domain via metalloproteases (MMPs), which include both MMP-9 and ADAM10. Adopted from Vazzana et al., 2009.

It has been shown that soluble RAGE formation occurs via its cytosolic cleavage by enzymes called metalloproteases. These extracellular enzymes employ metal ions, generally zinc, in its catalytic processes. Two of these enzymes, ADAM10 and MMP-9 (also known as gelatinase B), have been suspected to be the key force in the shedding of soluble RAGE from full length RAGE (Metz et al., 2012; Vazzana et al., 2009). In a 2008 study by Raucci et al., it was found that the total amount of soluble RAGE was not accounted for through gene expression, as determined by RNA levels HEK293 cells in vitro and Western blot analysis. Additionally, ADAM10 deficient cells overproduced full length RAGE and decreased amounts of the soluble form (Raucci et al., 2008). To

confirm this finding, ADAM10 transcripts were introduced into the deficient cells and soluble RAGE levels were restored. From this, the researchers concluded that membrane bound RAGE must be cleaved to create the levels of soluble RAGE seen in their experiments, pointing to ADAM10 as the key molecule involved in this transformation (Raucci et al., 2008).

The present study is focused on understanding the relationship between genomic variants Gly82Ser (exon 3 of *AGER*, within the active site of the v-domain) (Pettersson-Fernholm et al., 2003), T-374A and T-429C (both located in the 5' flanking region of *AGER*, which overlaps *PBX2*'s 3'UTR) and G1704T (located in intron 7 of *AGER*), with the variant alleles listed second (Hudson et al., 2001; Kalea et al., 2009), as critical regulators of NAFLD severity (

Figure 6). Additionally, a comparison of serum AGE levels in the patients with the diseases within the NAFLD spectrum was performed. Our findings may explain why a subpopulation of NAFLD patients may progress to NASH due to increased carbonyl stress.

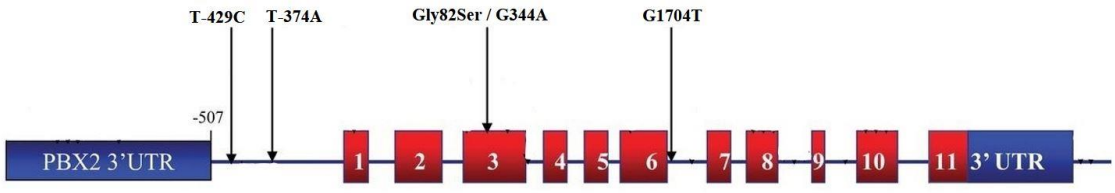

Figure 6 : Map of *AGER*'s commonly studied polymorphisms. As you can see, T-429C and T-374A are both in the 5' flanking region, which overlaps the 3'UTR region of PBX2. This area in AGER correlates to the gene's transcriptional start site. Gly82Ser (G344A) is a transition from a guanine, yielding a glycine residue, to an adenine, yielding a serine residue, in the third exon. This correlates to the active site of the RAGE protein. G1704T is found in intron 7, as noted above. The blue denotes 3'UTRs of both AGER and PBX2 and the red

denotes exons, numbered respectively. Additionally, arrows show areas of known polymorphisms, with the labeled polymorphisms being key to RAGE itself. Adopted from Hudson et al, 2001.

PRELIMINARY DATA

Total esRAGE levels were previously quantified in the lab, using ELISA. Analysis of this data showed no association between total levels of the soluble RAGE protein and the presence or absence of liver steatosis. In spring of 2016, analysis of non-synonymous SNP rs2070600 (Gly82Ser) was completed by Dr. Rohini Mehta. Three other DNA variants were profiled within the present study.

HYPOTHESIS

This study has been performed to investigate the validity of the following two hypotheses.

Hypothesis 1: Patients with a particular combination of alleles of the non-synonymous Gly82Ser variant, in exon 3, and/or the non-coding variants T-374A, T-429C, located in the 5' flanking region and G1704T, located in intron 7, may exhibit higher levels of AGE-RAGE interactions and may have higher prevalence of NASH.

Current research is unclear regarding the alleles and their potential correlation to fatty liver disease in regard to non-obese ethnically homogenous populations, but do explore these polymorphisms in type 1 diabetics, antioxidant status and/or diabetic complications (Hudson et al., 2001; Kalea et al., 2009; Pettersson-Fernholm et al., 2003). Although they have not been studied in a diverse, morbidly obese sample, or with a direct relation to NAFLD, these polymorphisms may also be risk factors of metabolic complications including inflammatory phenotype related to the AGE-RAGE axis in morbidly obese individuals.

Hypothesis 2: In serum samples of obese diabetic and/or NAFLD patients, the levels of glycations, as evident by the levels of AGE ligands, may be higher than that in obese, non-diabetic controls with healthy livers. Due to the increase of inflammatory

cytokines as a result of AGE-RAGE interactions, it is simplest to assume that AGE will be higher in patients with inflammatory diseases.

The serine mutation (AA genotype of Gly82Ser/G344A) increases the levels of MMPs released extracellularly, which would theoretically lead to an increase of esRAGE in individuals with the mutation. Although the esRAGE connection was not seen in the present data, an increase of ligand binding is likely to occur due to the inflammatory effects of an increase of AGE-RAGE interactions.

The polymorphisms within the 5' flanking region of *AGER* are more complex in their interpretation. *In vitro*, the T-429C variant correlates with an increase of transcription of AGER (Kalea et al., 2009). Additionally, it has been shown that the variant allele (-429C) was associated with insulin resistance and higher HbA_{1c} levels (Hudson et al., 2001; Kalea et al., 2009), yet the Kalea study was done with type 1 diabetic patients, a disease of a different origin than type 2 diabetic development, thus may come with different complications in regards to chronic inflammation associated with non-alcoholic fatty liver disease. Second, the T-374A variant correlates to increased gene expression *in vitro* (Hudson et al., 2001) yet terminated binding of transcription factors *in vivo* (Kalea et al., 2009), repressing RAGE transcription. On the surface, these results appear to contrast one another, yet the methods used may explain any inconsistencies of their evidence. Additionally, *in vivo* studies indicate that the variant allele (-374A) is protective against diabetic complications (Kalea et al., 2009) which may or may not include the chronic inflammation seen in morbid obesity and NAFLD. Further

studies are necessary to clarify the role of T-374A *in vivo* (Kalea et al., 2009) and in regards to RAGE and chronic inflammation of the liver in a morbidly obese population.

Lastly, the data concerning G1704T variant in intron 7 are limited. One study linked the common allele of G1704T (1704G) with increased serum antioxidants and decreased levels of glycations when this allele was combined with the A2184G variant of AGER (Mu and Stejskalov, 2001). Furthermore, in a study looking at the impact of alleles AGER G1704T and NADPH p22phox C242T, a connection of heterozygous and homozygous variant alleles of G1704T (1704GT and 1704TT) in combination to the common allele of NADH p22phox C242T (242CC) to diabetic nephropathy in type 2 diabetic patients was reported (Matsunaga-Irie et al., 2004). There is not much data on this SNP, but as one of the common polymorphisms of this gene and its partial association to complications of type 2 diabetes, a disease linked to morbid obesity and chronic inflammation, it is beneficial to analyze in the realm of this study.

Due to its role in inflammation, it is simplest to assume in the second hypothesis that patients with increased levels of inflammation, either in conjunction with type 2 diabetes or with NAFLD, will have higher levels of circulating AGE as compared to non-diabetic, non-NAFLD controls, assuming no other pathways are confounding the pro-inflammatory events of the AGE-RAGE interaction. As the preliminary data shows no increase of esRAGE in the groups studied, we can eliminate the confounding variable of esRAGE's function to clear AGE from circulation. Basic receptor-ligand kinetics state that an increase of ligand in absence of an increase of competitive inhibitors will increase the receptor-ligand binding overall, thus increasing receptor-ligand activation of

downstream events. In this case, an increase of AGE in absence of an increase of esRAGE, as seen in preliminary data, will increase the frequency of AGE-RAGE interactions, signaling downstream inflammatory events and an increase of RAGE expression due to positive feedback of this interaction.

STUDY AIMS

First, in the collection of DNA extracted from whole blood samples of obese patients with or without the type 2 diabetes and/or without the NAFLD, we aimed on genotyping and analyzing four single nucleotide polymorphisms located within the RAGE-encoding gene, *AGER* and analyzing based on fatty liver status. Next, in the same patients' cohorts, we aimed at accessing the levels of translated and secreted AGE protein by ELISA assays and correlating these levels with the levels of soluble RAGE. Last, we planned to uncover the correlation between RAGE genotypes, the total levels of circulating AGE ligand in sera, and the presence of specific forms of NAFLD and/or diabetes.

METHODS

This study has been approved by Internal Review Board of Inova Fairfax Hospital (Federal Assurance FWA00000573).

Study population

Fasting whole blood and liver tissue samples were collected from 340 morbidly obese patients (BMI ≥ 35) undergoing laparoscopic sleeve gastrectomy between the years of 2003 and 2012. All patients gave informed consent before biological samples were collected. In each sample, serum was separated and processed by standard procedure set forth by Inova Hospitals by a clinician, then immediately flash frozen in liquid nitrogen and added to the repository of specimens stored at −80° C. The samples were immediately frozen with liquid nitrogen and stored at −80 ºC until use. The samples were de-identified in compliance with HIPAA regulations. A liver biopsy was performed at the same time and histopathology was obtained for each sample. Clinical and laboratory variables from the time of surgery were extracted from medical records.

Racial demographics were self-reported. Out of 340 patients, there were 261 Caucasians, 50 African-Americans, and 12 Hispanics. Eight patients reported their race as "other" and for 9 patients, race was unknown. The mean age of these patients was 44.08 ± 11.25 years, with an average BMI being at 48.06 ± 9.08 kg/m^2. About a third of the cohort, 31.2%, had been diagnosed with type 2 diabetes. Likewise, approximately a

third had been diagnosed with NAFLD (30.6%) or NASH (30.3%), leaving 39.1% without current NAFLD diagnosis (Table 1). In all cases, NAFLD diagnosis was completed using biopsied tissue collected at the time of surgery. Tissue pathology was analyzed by histologist from INOVA Fairfax Hospital and given a score based on fat accumulation, fibrosis, and ballooning.

Table 1: Demographics of the genotyped cohort. A subset of these individuals also underwent circulating AGE ligand quantification via ELISA assay.

Variable (N=340)	Mean ± St. Dev. or % (N)
Age (years)	44.08 ± 11.25
BMI (kg/m2)	48.06 ± 9.08
Type 2 Diabetes	31.2% (N = 106)
No Non-alcoholic fatty liver disease (non-NAFLD)	39.1% (N = 133)
Non-alcoholic fatty liver disease (NAFLD)	30.6% (N = 104)
Non-alcoholic steatohepatitis (NASH)	30.3% (N = 103)

Inclusion criteria

Patients with hepatitis, HIV, or other viral chronic liver diseases were excluded from this study. Additionally, those patients who have had or currently have cancer were not included in this cohort. Those who consumed excessive amounts of alcohol (> 10 grams/day for females and > 20 grams/day for males) were also excluded.

Clinical samples

Previously collected whole blood samples and liver tissue biopsies were utilized for this study. Prior to the beginning of this study, total DNA was extracted from whole blood using QIAamp® kits in accordance with manufacturer's instructions (Qiagen, USA). DNA was then quantified and quality assessed by spectrophotometer (GeneQuant 1300, General Electric). Additionally, to assess the integrity of extracted DNA, agarose gel electrophoresis runs were carried out. The gels were inspected for evidence of poor DNA quality visible as degradation/smearing. Each DNA sample was diluted to a final concentration of 10 ng/uL, prior to use for the genotyping assays. This extraction was originally used for the preliminary esRAGE study in 2016 and was carried out by Dr. Rohini Mehta at Inova Fairfax Hospital.

AGER genotyping was performed in DNA extracted from whole blood PMBCs using the methods mentioned above. Quantification of circulating AGE ligands were performed in a subset of patients (N = 226) due to the lack of requested amount of serum from other samples. All samples were stored in -80 ºC until time of use.

AGER Polymorphism Genotyping

AGER polymorphism genotyping was completed by TaqMan qPCR. The *AGER* gene (an 11 exon, 3.27kb span on chromosome 6p21.3) was the focus of this study. Four SNPs, Gly82Ser (rs2070600), T-374A (rs1800624), T-429C (rs1800625), and G1704T (rs184003) were assayed. Patient whole-blood DNA from peripheral blood mononuclear

cells (PBMCs), diluted to 1:10 µL in nuclease free water, was used and aliquoted into 20 µL volumes in a 96-well plate. This dilution was created by first disinfecting the necessary tools used with a 70% ethanol solution. These tools and a new, clean 96-well plate were subject to ten minutes of UV exposure in a Labconco Purifier Class I Safety Exposure UV hood. Post UV disinfection, 18 µL of nuclease free water (Fisher Lot: 146653) was added into each well of the 96-well plate. Additionally, 2 µL of extracted patient's whole blood DNA was added into each well, following a premade key for the location of each sample. Care was taken to ensure no wells were contaminated by other patient samples. A micro-seal adhesive seal was added under the hood and sealed via light manual pressure to prevent evaporation. A total of six 96-well plates were prepared and placed in the 4 ºC freezer before use.

TaqMan qPCR with the Applied Biosystems TaqMan® Genotyping Master Mix (Part No: 371353, Lot: 1601042, Exp: 07 Mar 2017) was utilized for each of the six 96-well plates, prepared individually. Genotype-specific Assay Mixes were created for each of the 4 *AGER* polymorphisms by diluting the 40x stock to 20x in nuclease free water in a separate tube and stored at -20 ºC.

Pre-diluted whole blood DNA plates were spun down at 150g for five minutes before use and placed on ice. Pre-aliquoted samples of 20x genotype assay, 2x genotype-specific MasterMix, and nuclease free water (no DEPC) were allowed to cool/thaw on ice before use. The three solutions were spun down to join contents in a microcentrifuge. To create the MasterMix solution for the assay, 0.5 µL of 20x genotype assay mix, 5.0 µL 2x genotype MasterMix, and 3.5 µL of water were placed into each well of a new 96-well

plate. To this, 1 µL of pre-diluted DNA was individually added into each well of the new plate to create a total of 10 µL per well. No DNA was added into wells labeled "NTC". The new plate was then sealed with a micro-seal cover and spun down at 150g for one minute to join contents.

96-well TaqMan PCR was performed using BioRad CFX96 PCR instrument (Biorad, USA). The procedure was repeated for 40 cycles, consisting of 95 ºC (10min)/ 95 ºC (15s) denaturation /60 ºC (60s) annealing per cycle. Two fluorophores, VIC and FAM were utilized in determining which allele is present. From this, the alleles were determined via the amplification curves created using data collected at the end of each amplification step and visually read and verified in person to confirm results.

AGE Ligand Quantification

Quantification of the concentration of circulating advanced glycation end products (AGEs) has been completed via competitive ELISA assay. Cell Biolabs, Inc.'s OxiSelect™ Advanced Glycation End Product Competitive ELISA Kit (PN: STA-817 Lot: 10101323 Exp: 4/2017) was used to complete the six plates, in duplicate, using the manufacturer's protocol. A total of 226 samples of patient serum were aliquoted into 96-well plates, at 110 µL per sample, the plates were stored for use in the immediate future.

Conjugate diluent (Cell Biolabs, Inc. PN: 281603) was diluted from the stock 100x to 1x using 50 µL 100x Conjugate diluent in 4.95 mL 1x PBS (Gibco pH 7.2 -/- CaCl/MgCl; Ref: 20012-043 PN: 1715697). Next, 10 µg/mL AGE conjugate (Cell Biolabs, Inc. PN: 281702) was created using 50 µL of the stock 1 mg/mL AGE conjugate in 4.95 mL 1x PBS. These two 5 mL dilutions were added together and at a 1:1 ratio,

yielding a total of 10 mL. Using a multichannel pipette, 100 µL of this solution was added into each well of the sealed 96-well plate included in the kit. The plates were incubated overnight at 4 ºC.

Day two of the ELISA assay was started by creating AGE standards for each plate using the 1 mg/mL AGE-BSA standard included in the kit (Cell Biolabs, Inc. PN: 281703). The standard concentrations and dilutions can be found in Table 2. The ten standards were run in duplicate simultaneously with the samples of each plate. The values of these standards were used to create the standard curve used to find the concentrations of the samples in each plate.

Table 2 : The dilutions of circulating AGE standard and its concentrations using a 1 mg/mL AGE-BSA Standard (Cell Biolabs, Inc. PN: 281703).

Dilution #	1 mg/mL AGE-BSA Standard (µL)	Assay Diluent (µL)	AGE-BSA Final Concentration (µg/mL)
1	40	360	100
2	200 of #1	200	50
3	200 of #2	200	25
4	200 of #3	200	12.5
5	200 of #4	200	6.25
6	200 of #5	200	3.13
7	200 of #6	200	1.56
8	200 of #7	200	0.78
9	200 of #8	200	0.39
10	0	200	0

Once the standards were created, the AGE conjugate coated plate was removed from its storage at 4 ºC. The AGE Conjugate solution was removed and the plate was

washed out two times with 1x PBS using a clean wash bottle. The plate was blotted on clean paper towels before and after each wash to remove excess liquid. Next, 200 µL of assay diluent (Cell Biolabs, Inc. PN: 310804) was added into each well of the AGE conjugate coated plate and incubated at room temperature for one hour. After the incubation, the plate was aspirated and blotted before the next step. 50 µL of sample serum and standards were placed in duplicate in their respective, predetermined, wells in the AGE conjugate plate. This was incubated for ten minutes at room temperature on the orbital shaker set at 250 RPM. During this time, anti-AGE antibody was diluted to 1:1000 using 10 µL of 1000x anti-AGE antibody (Cell Biolabs, Inc. PN: 281701) in 9.99 mL assay diluent. Once the incubation was complete, 50 µL of the 1:1000 dilution of anti-AGE antibody was added into each well of the AGE conjugate plate atop the serum or standards already in the wells. This was allowed to incubate for one hour at room temperature on the orbital shaker set at 250 RPM. During this time, a 1:1000 dilution of the secondary antibody, HRP conjugate (Cell Biolabs, Inc. PN: 231704) was created by adding 20 µL of 1000x secondary antibody, HRP conjugate to 19.98 mL assay diluent. Additionally, 1x wash buffer was created by diluting 100 mL of 10x wash Buffer (Cell Biolabs, Inc. PN: 310806) in 900 mL deionized water.

After the one hour incubation with the anti-AGE antibody, the serum-antibody solution was removed and the plate was washed 3x with 250 µL 1x wash buffer, blotting the plate with clean paper towels before and after each wash. The washed plate then received 100 µL of freshly diluted 1:1000 secondary antibody, HRP conjugate into each well. The plate was then incubated for one hour at room temperature on the orbital shaker

set at 250 RPM. After this incubation, the plate was aspirated and again washed 3 times with 250 µL 1x Wash buffer, blotting the plate with clean paper towels before and after each wash.

After blotting the plate, 100 µL room temperature substrate solution (Cell Biolabs, Inc. PN: 310807) was added into each well. Substrate solution was allowed to develop for seven minutes before the reaction was stopped (Cell Biolabs, Inc. PN: 310808). Each plate was read using a plate reader with 450nm as the primary wavelength. Circulating AGE concentrations recorded in µg/mL.

Statistical Analysis

Basic descriptive statistics were completed using Microsoft Excel and SPSS 24.0. This includes gender and race data, average BMI, age, diabetes, and NAFLD/NASH numbers.

In all cases, results are considered significant at $P < 0.05$.

Statistical analysis was performed using the SPSS software package (SPSS 24.0, licensed to George Mason University) and R. Continuous variables were expressed as the mean ± SD. Categorical variables were presented as frequencies. Group differences were analyzed by the Mann-Whitney test, as it is assumed that this extreme weight class is not normally distributed. For genotypic and allelic frequencies, the Hardy-Weinberg equilibrium (Table 3; Table 4; Table 5) was applied using SNPStats online tools with the assistance of Dr. Rohini Mehta and Munkhzul Otgonsuren of Inova Health Systems in Fairfax, VA. Univariate analysis and multiple logistic regression analysis were performed for haplogroup assessment of RAGE variants and RAGE protein levels in the subjects.

An alpha value of < 0.05 was considered statistically significant for all analyses. Four group comparisons were performed: 1) NASH (N=103) vs all other groups (N=237), 2) NASH (N=103) vs Mild abnormal and No disease (N=133), 3) NASH (N=103) vs No disease (N=94), and 4) NASH (N=103) vs NAFLD (N=104). Individual SNP analysis was done using a Kruksal-Wallis test separating based on fatty liver status. Haplotype analysis was done using the haplo.stats program in R separated based upon fatty liver status.

Table 3 : SNP genotyping data (n=340). The common homozygous alleles are listed first, with the heterozygote in the middle and the variant homozygote listed last for each SNP.

Gly82Ser/ G344A (rs2070600)	
GG	311
GA	29
AA	0
G1704T (rs184003)	
GG	281
GT	54
TT	5
T-374A (rs1800624)	
TT	213
AT	111
AA	16
T-429C (rs1800625)	
TT	237
CT	91
CC	12

The levels of circulating AGEs were analyzed using SPSS 24.0 licensed to George Mason University. Mann-Whitney tests were applied to various comparisons

between following groups: 1) NAFLD, 2) NASH, 3) Mild Abnormality of Liver Parenchyma, and 4) No Disease. Histopathological diagnosis defined no disease as patients with minimal steatosis and no inflammation. Mild abnormality of liver parenchyma referred to patients with less than 5% fat accumulation (steatosis) in biopsied tissue and/or inflammation not related to NAFLD. Both NAFLD and NASH patients show signs of steatosis (≥ 5% fat accumulation). NAFLD patients also have lobular inflammation and/or portal inflammation (immune cell infiltration) in their histopathological records, whereas NASH patients have inflammation as well as ballooning degeneration of hepatocytes, pericellular fibrosis and/or presence of Mallory-Denk bodies. Additionally, each group of patients was split into subgroups with and without type 2 diabetes, for diabetes-specific analysis. Diabetic status was pre-diagnosed and reported on a yes/no basis. Additional diabetic testing was not done in the scope of this study.

RESULTS

AGER Haplotype Analysis

In patients with NASH (N=103), histopathologically diagnosed as ones with presence of fat, ballooning, Mallory-Denk bodies, and pericellular fibrosis the T-A-G-G haplotype (

Haplotype	No Disease (N=94)	Mild Abnormal (N=39)	NAFLD (N=104)	NASH (N=103)	All (N=340)
TTGT	18	7	20	11	56
TTGG	112	47	130	123	412
TTAT	0	2	1	0	3
TTAG	10	3	7	10	30
TAGT	4	2	11	6	23
TAGG	34	16	38	51	139
TAAT	0	0	0	0	0
TAAG	1	0	0	2	3
CTGT	4	2	5	1	12
CTGG	28	10	30	33	101
CTAT	0	0	0	0	0
CTAG	3	1	2	3	9
CAGT	2	0	1	2	5
CAGG	7	1	9	9	26
CAAT	0	0	0	0	0
CAAG	0	0	0	0	0

Table 6**)** was more prevalent as compared to all other groups combined (NAFLD, Mild abnormal, and no disease) (N=237; $P \leq 0.05$), with a haplotype score of 2.46. Additionally, the T-A-G-G haplotype had a higher significance than in patients with NASH (N=103) as compared to those with no disease (N=94; $P \leq 0.01$) with a haplotype score of 2.72 (Table 7). The T-A-G-T haplotype was more prevalent in patients with NASH (N=103) as compared to those with Mild Abnormality of Liver Parenchyma and No Disease combined (N=133; $P \leq 0.01$), with a haplotype score of 2.60 (

Hap-Score	T-429C	T-374A	Gly82Ser	G1704T	P-value
-1.7555	T	T	G	T	0.079175
-1.63741	T	T	G	G	0.101544
-0.26852	T	T	A	G	0.788298
0.81318	C	T	G	G	0.416115
2.60645	T	A	G	T	0.009149

Table 8). There were no differences in prevalence of these two genotypes, when NASH patients (N=103) were compared to those with non-NASH NAFLD (N=104).

Haplotype scoring was computed using a built-in algorithm in the Haplo.stats statistical package in R and completed with the assistance of Dr. Rohini Mehta and Munkhzul Otgonsuren of Inova Health Systems in Fairfax, VA (Schaid et al., 2002). This program has been designed to use the maximum likelihood model to determine haplotype association between disease and genotype. Due to allelic combinations and the uncertainties that may arise due to heterozygotes in various loci, patients with known haplotypes were those homozygotes for all four SNPs, and those heterozygous for one of the four SNPs tested. Those individuals who were heterozygotes in two or more of the

four SNPs tested were interpreted as having more than one haplotype, which is accounted for in the statistics of this program (Schaid et al., 2002). The program assumes the data meets Hardy-Weinberg equilibrium, which was consistent in our dataset in all cases (Table 4). The functions used were hap.score to determine the haplotype score statistic and the p value of this score, pool.hf to determine the haplotype frequency of the pooled sample, control.hf and case.hf to determine the haplotype frequencies for the control/case sample only, glm.eff to determine if the haplotype was modeled as an effect, part of the baseline, or a rare haplotype in the population overall. Additionally, odds ratios, or the effects sizes of the haplotypes assuming haplotype effects were multiplicative, were calculated using OR.upper and OR.lower.

For all the haplotypes analyzed, a positive haplotype score correlates to an increased frequency of that particular haplotype in case diagnoses (Schiad et al., 2002), which was NASH in all cases. As seen in Table 6, Table 7, and Table 8, the significant haplotype scores were all positive, thus showing a possible correlation between these haplotypes and risk of NASH development in a morbidly obese population.

Table 4: Frequency table of all patients with Hardy-Weinberg χ^2 values. Both allele frequency and genotype frequency are reported, using the "=CountIf" function in Microsoft excel for genotype and the formula (allele frequency) = 2*(homozygote)+(heterozygote) for alleles.

Frequency table - All patients (N=340)				
T-429C [rs1800625]				
	No Disease (N=94)	**Mild Abnormal (N= 39)**	**NAFLD (N=104)**	**NASH (N=103)**
	Allele Frequency			
T	159	66	174	170
C	29	12	34	36
	Genotype Frequency			
TT	69	29	73	70
TC	21	8	28	30
CC	4	2	3	3
Heterozygosity	0.26	0.26	0.27	0.29
HWE χ2, 1 D.F.	1.94	1.75	0.03	0.01
Meets HWE, Y/N	Y	Y	Y	Y
T-374A [rs1800624]				
	No Disease (N=94)	**Mild Abnormal (N= 39)**	**NAFLD (N=104)**	**NASH (N=103)**
	Allele Frequency			
T	159	61	167	151
A	29	17	41	55
	Genotype Frequency			
TT	68	25	67	54
TA	23	11	33	43
AA	3	3	4	6
Heterozygosity	0.26	0.34	0.32	0.39
HWE χ2, 1 D.F.	0.36	1.16	0.00	0.46
Meets HWE, Y/N	Y	Y	Y	Y
Gly82Ser / G344A [rs2070600]				
	No Disease (N=94)	**Mild Abnormal (N= 39)**	**NAFLD (N=104)**	**NASH (N=103)**
	Allele Frequency			
G	179	79	201	198
A	9	3	7	8
	Genotype Frequency			
GG	85	36	97	95
GA	9	3	7	8
AA	0	0	0	0
Heterozygosity	0.09	0.07	0.07	0.07
HWE χ2, 1 D.F.	0.24	0.06	0.13	0.17
Meets HWE, Y/N	Y	Y	Y	Y
G1704T [rs184003]				
	No Disease (N=94)	**Mild Abnormal (N= 39)**	**NAFLD (N=104)**	**NASH (N=103)**
	Allele Frequency			
G	168	69	185	192
T	20	9	23	14
	Genotype Frequency			
GG	75	31	82	90
GT	18	7	21	12
TT	1	1	1	1
Heterozygosity	0.19	0.20	0.20	0.13
HWE χ2, 1 D.F.	0.00	0.57	0.07	0.67
HWE at $\alpha_{=0.05}$, Y/N	Y	Y	Y	Y

Table 5 : The number of patients in each haplotype divided by liver histopathology. The SNPs are listed in genetic map order of the *AGER* gene (T-429C, T-374A, Gly82Ser/G344A, and G1704T), and haplotypes are listed in reverse alphabetical order. Haplotypes of homozygotes were counted twice and haplotypes of heterozygotes were counted once for each of the possible combinations of alleles. There were no quadruple

heterozygotes in this patient cohort. In the case of double and triple heterozygotes, the program haplo.stats uses a likelihood ratio to determine probability of each possible haplotype, thus, numbers shown here are not reflective of the real number values used by the program for calculations (Schaid et al., 2002). Shown here are the sum of all possible haplotypes in the patients studied (N=340).

Haplotype	No Disease (N=94)	Mild Abnormal (N=39)	NAFLD (N=104)	NASH (N=103)	All (N=340)
TTGT	18	7	20	11	56
TTGG	112	47	130	123	412
TTAT	0	2	1	0	3
TTAG	10	3	7	10	30
TAGT	4	2	11	6	23
TAGG	34	16	38	51	139
TAAT	0	0	0	0	0
TAAG	1	0	0	2	3
CTGT	4	2	5	1	12
CTGG	28	10	30	33	101
CTAT	0	0	0	0	0
CTAG	3	1	2	3	9
CAGT	2	0	1	2	5
CAGG	7	1	9	9	26
CAAT	0	0	0	0	0
CAAG	0	0	0	0	0

Table 6 : Comparative analysis of haplotypes in NASH (N = 103) vs non-NASH (N = 237) cohorts using Haplo.stats in R. The highlighted row indicates a significant p-value. Haplotypes not included denotes a haplotype that did not have enough patients to be compared in either case or control group.

Hap-Score	T-429C	T-374A	Gly82Ser	G1704T	P-value
-1.773868	T	T	G	T	0.076085
-1.282937	T	T	G	G	0.199514
-0.077783	T	T	A	G	0.938001
0.423045	T	A	G	T	0.672263
0.593927	C	T	G	G	0.552561
2.416798	T	A	G	G	0.015658

Table 7 : Comparative analysis of haplotypes in NASH (N = 103) vs No Disease (N = 94) cohorts using Haplo.stats in R. The highlighted row indicates a significant p-value. Haplotypes not included denotes a haplotype that did not have enough patients to be compared.

Hap-Score	T-429C	T-374A	Gly82Ser	G1704T	P-value
-1.7555	T	T	G	T	0.079175
-1.63741	T	T	G	G	0.101544
-0.26852	T	T	A	G	0.788298
0.81318	C	T	G	G	0.416115
2.60645	T	A	G	T	0.009149

Table 8 : Comparative analysis of haplotypes in NASH (N = 103) and a cohort with Mild Abnormality of liver Parenchyma and No disease combined (N = 133) using Haplo.stats in R. The highlighted row indicates a significant p-value. Haplotypes not included denotes a haplotype that did not have enough patients to be compared.

Hap-Score	T-429C	T-374A	Gly82Ser	G1704T	P-value
-1.7555	T	T	G	G	0.079175
-1.63741	T	T	G	T	0.101544
-0.26852	T	T	A	G	0.788298
0.81318	C	T	G	G	0.416115
2.60645	T	A	G	T	0.009149

Table 9 : Individual SNP association tests. Both Kruskal-Wallis tests and Chi-squared tests for association were completed using individual SNP data. No single allele of the studied *AGER* polymorphisms was found to be significant in the determination of liver histopathology in the cohort tested.

Individual SNP Association Tests - All patients (N=340)				
T-429C [rs1800625]				
	No Disease (N=94)	**Mild Abnormal (N= 39)**	**NAFLD (N=104)**	**NASH (N=103)**
	Kruskal-Wallis Test			
Average Rank	170	164.2	169.9	174
Z	-0.06	-0.43	-0.08	0.44
	P = 0.960; Adjusted for ties P = 0.925			
	Chi-Square Test for Association: Count[Expected]			
TT	66[65.80]	29[27.30]	73[72.80]	70[72.10]
TC	25[24.88]	8[10.32]	28[27.53]	29[27.26]
CC	3[3.32]	2[1.38]	3[3.67]	4[3.64]
	Pearson Chi-square = 1.282, DF = 6, P = 0.973			
T-374A [rs1800624]				
	No Disease (N=94)	**Mild Abnormal (N= 39)**	**NAFLD (N=104)**	**NASH (N=103)**
	Kruskal-Wallis Test			
Average Rank	162.6	169.6	166.6	182
Z	-0.91	-0.06	-0.49	1.42
	P = 0.539; Adjusted for ties P = 0.391			
	Chi-Square Test for Association: Count[Expected]			
TT	63[58.61]	25[24.32]	67[64/85]	57[64.22]
TA	27[30.96]	11[12.85]	33[34.26]	41[33.93]
AA	4[4.42]	3[1.84]	4[4.89]	5[4.85]
	Pearson Chi-square = 4.472, DF = 6, P = 0.613			
Gly82Ser / G344A [rs2070600]				
	No Disease (N=94)	**Mild Abnormal (N= 39)**	**NAFLD (N=104)**	**NASH (N=103)**
	Kruskal-Wallis Test			
Average Rank	174.1	169.1	167.4	170.9
Z	0.42	-0.1	-0.38	0.04
	P = 0.972; Adjusted for ties P = 0.800			
	Chi-Square Test for Association: Count[Expected]			
GG	84[85.982]	36[35.674]	97[95.129]	94[94.215]
GA	10[8.018]	3[3.326]	7[8.871]	9[8.785]
AA	0[0]	0[0]	0[0]	0[0]
	Pearson Chi-square = 1.008, DF = 3, P = 0.799			
G1704T [rs184003]				
	No Disease (N=94)	**Mild Abnormal (N= 39)**	**NAFLD (N=104)**	**NASH (N=103)**
	Kruskal-Wallis Test			
Average Rank	173.7	176.1	176.7	159.2
Z	0.37	0.38	0.77	-1.4
	P = 0.570; Adjusted for ties P = 0.199			
	Chi-Square Test for Association: Count[Expected]			
GG	76[77.688]	31[32.232]	82[85.953]	92[85.126]
GT	16[14.929]	7[6.194]	21[16.518]	10[16.359]
TT	2[1.382]	1[0.574]	1[1.529]	1[1.515]
	Pearson Chi-square = 5.642, DF = 6			

ELISA profiling in AGE proteins

Cohort-specific serum concentrations of AGE ligand were compared by non-parametric Mann-Whitney tests. The cohorts were selected according to histopathological findings in their liver biopsies (

Table 11;

Table 12), along with presence or absence of type 2 diabetes (

Table 12;

Table 13). When the group of patients diagnosed as having "mild abnormalities in liver parenchyma" was compared to the group with no detectable liver disease, a significant difference between median values of circulating AGE concentration was detected, with a lower AGE value in those in the mild abnormal group, contradicting my second hypothesis (

Table 11; $P \leq 0.05$). None of the other possible comparisons showed significant differences between median circulating AGE concentration levels.

Table 10 : Average circulating AGE levels based on liver histopathology and diabetic status. Circulating AGE averages are listed in µg/mL and N is in brackets.

	Overall (µg/mL) Mean ± st. dev [N]	**Type 2 Diabetics (µg/mL) Mean ± st. dev [N]**	**Non-diabetics (µg/mL) Mean ± st. dev [N]**
No disease	10.37 ± 4.68 [67]	10.63 ± 4.41 [16]	10.29 ± 4.80 [51]
Mild Abnormal	8.50 ± 4.95 [32]	7.55 ± 3.91 [7]	8.77 ± 5.24 [25]
NAFLD	9.70 ± 4.63 [68]	8.96 ± 4.15 [26]	10.16 ± 4.89 [42]
NASH	10.14 ± 5.31 [59]	10.59 ± 5.12 [24]	9.82 ± 5.48 [35]

Table 11 : The results of group comparisons for amounts of circulating AGE levels in patient sera. Patients with and without type 2 diabetes are included in combination in this report. The highlighted row indicates a significant p-value. Bold groups indicate lower averages in each comparison. P-values calculated using Mann-Whitney testing. See table 7 for average circulating AGE in each grouping.

Comparisons (N=226)	**P-value**
NASH (N=59) vs **NAFLD** (N=68)	0.772
NASH vs **Mild Ab.** (N=32)	0.114
NASH vs No dis. (N=67)	0.569
NASH (N=59) vs **All others** (N=167)	0.757
NASH vs **Mild Ab. + No Dis**. (N=99)	0.792
NASH vs **NAFLD + Mild Ab**. (N=100)	0.373

NAFLD vs **Mild Abnormalities**	0.174
NAFLD vs No Disease	0.358
Mild Abnormalities vs No Disease.	0.040

Table 12 : The results of group comparisons for amounts of circulating AGE levels in patient sera diagnosed with diabetes. There were no significant differences in circulating AGE levels within this subgroup of patients. Bold groups indicate lower averages in each comparison. P-values calculated using Mann-Whitney testing. See table 7 for average circulating AGE in each grouping.

Type 2 Diabetics (N=72)	**P-value**
NASH (N=24) vs **NAFLD** (N=26)	0.260
NASH vs **Mild Ab**. (N=7)	0.143
NASH vs No dis. (N=16)	0.934
NASH vs **All others** (N=49)	0.313
NASH vs **Mild Ab. + No Dis**.(N=23)	0.551
NASH vs **NAFLD + Mild Ab.** (N=33)	0.150
NAFLD vs **Mild Ab.**	0.403
NAFLD vs No dis.	0.223
Mild Abnormalities Vs No disease	0.095

Table 13 : The results of group comparisons for amounts of circulating AGE levels in patient sera in patients with non-impaired sugar metabolism. There were no significant differences in circulating AGE levels within this subgroup of patients. Bold groups indicate lower averages in each comparison. P-values calculated using Mann-Whitney testing. See table 7 for average circulating AGE in each grouping.

Non diabetics (N=153)	**P-Value**
NASH (N=35) vs NAFLD (N=42)	0.609
NASH vs **Mild Ab.** (N=25)	0.440
NASH vs No dis. (N=51)	0.447
NASH vs All others (N=118)	0.712

NASH vs **Mild Ab. + No Dis**. (N=76)	0.824
NASH vs **NAFLD + Mild Ab.** (N=67)	0.992
NAFLD vs **Mild Ab.**	0.204
NAFLD vs No dis.	0.850
Mild Abnormalities Vs No disease	0.134

DISCUSSION

About 35% of the American population is obese (BMI > 30.0 kg/m^2), and a comparable proportion is overweight (BMI between 25.0 kg/m^2 and 30.0 kg/m^2) (Garnett et al., 2016; Nagendran et al., 2016; Ogden et al., 2015). Obesity is delineated into three classes: Class I (BMI greater than or equal to 30.0 kg/m^2 and less than 35.0 kg/m^2), Class II or severe obesity (BMI greater than or equal to 35.0 kg/m^2 and less than 40.0 kg/m^2), and Class III or morbid obesity (BMI ≥ 40.0kg/m^2) (Sturm and Hattori, 2012). This study was performed in morbidly obese cohorts, also known as Class III obesity. Current assessment (2010) estimates that about 6.55% of the general U.S. population falls in the morbidly obese range, thus showing rapid increase from the 3.90% a decade before (Cusi, 2016; Kang et al., 2012; Piperi et al., 2015).

The relationship between type 2 diabetes, NAFLD, and obesity is well recognized (Kierdorf and Fritz, 2013; Oliveira et al., 2013; Ott et al., 2014; Ramasamy et al., 2009). The common theme among these three diseases is in their relation to systemic inflammation (see RAGE Interactions with AGE). The AGE-RAGE interactions trigger a signaling cascade that leads to an increase in secretion of inflammatory cytokines. Activation of AGE–RAGE interaction promotes NADPH-oxidase activity, resulting in activation of Nf-κB. AGE binding to RAGE also mediates the signaling through Janus

kinase (JAK) and signal transducers and activators of transcription (STATs) (Basaranoglu, 2011).

The data previously collected in our lab, failed to confirm an association between total levels of RAGE (P = 0.2879) and esRAGE (P = 0.1359) molecules with the presence or absence of Gly82Ser variant in patient DNA (Table 14). In fact, the only significant association of Gly82Ser variant was with the presence of Mallory-Denk bodies in liver biopsy in those with the variant allele, A (P = 0.0491; Table 14). The extent of this histopathological feature in a stained slice of biopsied tissue is proportional to the severity of the fatty liver disease in a patient (Preacher et al., 2005). Therefore, in current study, we expanded into an assessment of other variants located within *AGER* gene, which encodes RAGE isoforms. Three additional SNPs were studied: T-374A and T-429C, located in the 5' flanking region, and G1704T, located in intron 7 of the *AGER* gene. In the same cohort of patients, a substantially more powerful haplotype analysis was performed. By comparing the results of TaqMan qPCR genotyping assays with histopathological tissue assessments, two haplotypes were found to be significantly associated with liver pathology. The haplotype T-429 – A-374 – G344(Gly82) – G1704 was significantly overrepresented in the NASH cohort as compared to morbidly obese patients with healthy livers (P = 0.0064) and to all non-NASH patients (P=0.016). Additionally, the haplotype T-429 – A-374 – G344(Gly82) – T1704 was significantly overrepresented in those with NASH as compared to those with mild abnormalities in liver parenchyma and morbidly obese patients with healthy livers combined (P=0.01). No differences were found between patients with NASH and Non-NASH NAFLD.

Additionally, to determine if one polymorphism had a deterministic effect in the histopathology of patient livers, individual SNP associations were analyzed using Kruskal-Wallis and Chi-squared tests for association. Individually, no SNP was found to be significant in the patient cohort studied (Table 9). Because of this, one may assume that the combination of alleles has more influence in chronic inflammation in regard to liver histopathology than the individual SNPs themselves.

Table 14 : Total RAGE and esRAGE levels in patient sera and their relationships to the presence of Gly82Ser/ G344A variant. Data collected by Dr. Rohini Mehta of Inova Fairfax Hospital, 2016. The highlighted row indicates a significant p-value, calculated using Mann-Whitney analysis. The First numbers are the mean, the value in parenthesis is the range, and the square brackets denote the N of each variable.

Variable	Gly82Ser/G344A GG (N = 311)	Gly82Ser/G344A GA (N = 29)	P-value
Total esRAGE, ng/mL	0.20 (0.15-0.27) [131]	0.17 (0.11-0.23) [12]	0.1359
Total RAGE, pg/mL	925.63 (620.07-1360.07) [131]	702.20 (612.83-1134.69) [12]	0.2879
NASH/NAFLD status, N (%)			
No disease	85 (27.3%)	9 (31.0%)	
Mild abnormality of liver parynchema	35 (11.3%)	4 (13.8%)	
Non-NASH NAFLD	96 (30.9%)	8 (27.6%)	
NASH	95 (30.5%)	8 (27.6%)	
Age, years	44.00 (36.00-53.00) [311]	45.00 (39.00-52.00) [29]	0.8188
BMI	45.87 (41.89-52.10) [306]	47.91 (42.30-51.89) [28]	0.4666
White Blood cells	7.50 (6.30-9.20) [309]	8.40 (5.99-9.40) [29]	0.6528
Albumin	4.10 (3.90-4.30) [304]	4.10 (4.00-4.30) [27]	0.8142
Platelets	279.00 (239.00-336.00) [303]	270.00 (242.00-299.00) [29]	0.3996
Glucose	97.00 (87.00-116.50) [292]	97.00 (89.00-112.00) [26]	0.9211
ALT	28.00 (19.00-40.00) [307]	27.00 (18.00-37.00) [27]	0.4996
AST	22.00 (17.00-29.00) [307]	21.00 (16.00-24.00) [27]	0.2352
Triglycerides	138.00 (102.00-185.00) [279]	145.00 (115.00-174.00) [22]	0.8052
LDL	105.00 (86.00-128.00) [250]	107.50 (78.00-127.50) [20]	0.5218
Total cholesterol	189.00 (160.00-213.00) [283]	182.50 (155.00-199.00) [22]	0.3736
HDL	46.00 (39.00-55.00) [255]	45.50 (42.00-56.00) [20]	0.8794
Maximum number of medications	5.00 (2.00-7.00) [304]	6.00 (2.00-9.00) [25]	0.4088
Male	76 (24.4%)	10 (34.5%)	0.2340
White	234 (75.2%)	26 (89.7%)	0.0801
Presence of Mallory bodies (%)	274 (88.1%)	29 (100.0%)	0.0491

Notably, the differences in the prevalence of haplotypes were detectable only in so called “comparisons of the extremes”. This statistical method, known as the extreme groups approach (EGA), is typically used with data with at least one continuous variable, and aims to increase statistical power and reliability in the subsequent results (Preacher et al., 2005). The extremes are generally selected by taking the upper and lower quartiles in either the experimental data or population, and removing the middle values. This allows a clear comparison between those that clearly are, and those that clearly are not (Leslie et al., 2003). In the current study, the extremes were defined as those who possess NASH, and those who do not, excluding patients with non-NASH types of NAFLD. This allows evaluation of the pathophysiological components of the well-developed disease phenotype at the later stages of NAFLD progression, but does not shed the light at early stages of NAFLD, in particular, to the development of steatosis.

The first hypothesis of this study was that a particular haplotype of the non-synonymous SNP Gly82Ser/G344A, in exon 3, and/or the non-coding SNPs T-374A, T-429C, located in the 5’ flanking region and G1704T, located in intron 7, would exhibit a higher level of AGE-RAGE interactions, which may increase the likelihood of exhibiting a disease associated with chronic inflammation, namely non-alcoholic fatty liver disease. Additionally, the alleles T-429, T-374, and Gly82/G344 showed significant association with liver disease phenotypes in all three comparisons. The difference between the two significant haplotypes was in the G1704T polymorphism, which may point towards it’s insignificance in the receptor’s role in inflammation. The small patient haplotype numbers (Table 5) should be noted that the significant haplotype T-429 - T-374 -

Gly82/G344, - T1704 in the NASH vs mild abnormality of liver parenchyma and no disease (Table 8), which may disappear with a larger sample size. Moreover, the common alleles may be the driving factor to the link in haplotype to inflammation. This should be explicitly explored in additional studies. More studies need to be done to confirm this assumption, as well as analysis of the three static polymorphisms of these significant haplotypes. Nevertheless, in diabetes-specific analyses, these correlations were not replicated, possibly due to a lack in statistical power. Therefore, we should conclude that collected data does not support the hypothesis proposed.

The second hypothesis stated that in serum samples of obese diabetic and/or NAFLD patients, the levels of protein glycations as evident by the AGE levels would be higher than that in obese patients without NAFLD. However, the results of AGE-specific ELISA assays showed no differences between patients with NASH or NAFLD and all other groups regardless of their further parsing the subgroups with and without type 2 diabetes (

Table 11;

Table 12;

Table 13). Nevertheless, a comparison of serum samples collected from those with mild abnormalities in liver parenchyma versus morbidly obese patients with healthy livers showed significant differences in AGE levels ($p = 0.04$;

Table 11), indicating that the levels of AGE may, potentially, may not contribute to very early stages of liver disease, as the result is in the wrong direction (Table 11). It is important to note, though, that this correlation was not replicated, when same comparison was performed separately, when patients were separated into diabetics and these without type 2 diabetes. This indicates that observed correlation may be spurious.

In genome-wide association studies, AGEs levels in the blood were found to be highly heritable (Adams et al., 2016). However, when haplotypes were partitioned into individual SNPs, none of the candidate variant alleles were significantly associated. Instead, this study assessed each polymorphism individually, allowing us to obtain data on the genotype of each patient This strengthens the conclusion of this niche group of morbidly obese individuals, and aims to minimize any statistical issues that may arise from the small cohort of 340 patients.

Furthermore, rs1035798 in intron of the gene *AGER*, which was not profiled in this study, was recently shown to yield the highest significance in association with AGE levels (p=0.007), hinting towards the importance of introns, especially those close to the ligand binding domain(Adams et al., 2016), despite it being a synonymous SNP. Importantly, both the present study and that of Adams 2016, there is an investigation of global AGE levels; however, AGEs are a diverse set of molecules, either proteins or lipids, or both, that become glycated resulting from exposure to sugars. Direct quantification for each type of glycated product, separately, may lead to better delineation of AGE genetics. Alternatively, an increase in sample size may yield stronger results.

CONCLUSION

This study aimed to shed light on the association between systemic inflammation of morbidly obese population and the AGE-RAGE interaction, in hopes of determining differences between patients with various types of non-alcoholic fatty liver disease. Haplotype analysis for gene *AGER*, which encodes RAGE receptor, yielded no significant results. However, within this NAFLD cohort, we found a link between the *AGER* polymorphism Gly82Ser (G344A) and presence of Mallory-Denk bodies. Second, circulating AGE levels in patient sera were not related to presence or absence of the diagnosis of diabetes and/or particular type of non-alcoholic fatty liver disease. This conclusion was further solidified when analyses were performed separately in cohorts of patients divided into those with type 2 diabetes and those without.

To clarify the very much unclear role of AGE-RAGE interactions in the development of NAFLD, follow-up studies should further extend the cohorts profiled, and consider additional variables. This includes, but is not limited to, the medications each patient is taking, as they may alter the transcription levels of the *AGER* gene and/or alter pathogenesis of NAFLD. Future studies should also test diabetic status in house and diagnose patients using blood tests which reflect overall glucose level control, such as HbA_{1c}. In current study, the glucose control status of patients was not known. Additionally, patients who are diagnosed diabetics are more than likely on some type of

medication which may alter AGE levels or RAGE transcription. From this, a comparison of extremes should be done to clarify exactly what is occurring between diabetic and non-diabetic morbidly obese individuals in this cohort. Furthermore, patient diets should be surveyed, as literature shows that an intake of AGE with the diet may have significant role in defining circulating AGE levels and AGE-RAGE interactions *in vivo*.

Another interesting spin on this outcome is to explore the importance of the ligand concentration vs receptor architecture. Due to the absence of correlation between AGE levels and histopathological diagnosis, the receptor architecture may be more influential in morbidly obese individuals. At this stage of obesity, one may assume these individuals are living on a Western diet high in AGEs, as well as having other diseases related to obesity and metabolic syndrome that will increase the number of glycations. Because of this, the configuration of *AGER* may be the deciding factor between those who develop fatty livers and those who do not. Short of highly controlled animal studies, an increased sample size may tease apart this issue and shed some light upon this assertion.

In conclusion, despite the complexities of this ligand-receptor pair, AGE-RAGE interactions may contribute to progression to NASH in a subset of NAFLD patients. The lab has previously shown that there are no significant differences associated with clinical diagnosis of non-alcoholic fatty liver disease in either full length RAGE, whose primary function in this context is to interact with AGE and trigger inflammation, or esRAGE, the decoy receptor that acts to clear excess AGE from circulation. However, more studies are necessary before RAGE-AGE signaling disruptors, acting as inhibitors to ligand binding

on full length RAGE, may be recommended as therapeutic interventions designed to prevent and reverse the damage to the liver inflicted by chronic hyperglycemia or increased intake of dietary AGE as a result of food preparation (i.e. broiling).

REFERENCES

Adams, J.N., Raffield, L.M., Martelle, S.E., Freedman, B.I., Langefeld, C.D., Carr, J.J., Cox, A.J., and Bowden, D.W. (2016). Genetic analysis of advanced glycation end products in the DHS MIND study. Gene *584*, 173–179.

Baršić, N, Lerotić, I, and Smirčić-Duvnjak, L (2012). Overview and developments in noninvasive diagnosis of nonalcoholic fatty liver disease. World Journal of Gastroenterology, *18* (30). pp. 3945-54. ISSN 1007-9327.

Basaranoglu, M. (2011). Mallory-Denk Bodies in chronic hepatitis. World J Gastroentero *17*, 2172.

Cusi, K. (2016). Treatment of patients with type 2 diabetes and non-alcoholic fatty liver disease: current approaches and future directions. Diabetologia *59*, 1112–1120.

Ding, Q., and Keller, J. (2005). Evaluation of rage isoforms, ligands, and signaling in the brain. Biochimica et Biophysica Acta (BBA) - Molecular Cell Research *1746*, 18–27.

Garnett, S., Baur, L., Jones, A., and Hardy, L. (2016). Trends in the Prevalence of Morbid and Severe Obesity in Australian Children Aged 7-15 Years, 1985-2012. Plos One *11*, e0154879.

Gitto, S, Vukotic, R, Vitale, G, Pirillo, M, and Villa, E (2016). Non-alcoholic steatohepatitis and liver transplantation. Digestive and Liver Disease, *48*, (6). 587-591, ISSN 1590-8658.

Goldberg, T., Cai, W., Peppa, M., Dardaine, V., Baliga, B., Uribarri, J., and Vlassara, H. (2004). Advanced glycoxidation end products in commonly consumed foods. J Am Diet Assoc *104*, 1287–1291.

Henao-Mejia, J., Elinav, E., Jin, C., Hao, L., Mehal, W.Z., Strowig, T., Thaiss, C.A., Kau, A.L., Eisenbarth, S.C., and Jurczak, M.J. (2012). Inflammasome-mediated dysbiosis regulates progression of NAFLD and obesity. Nature *482*, 179–185.

Hudson, B.I., Stickland, M.H., Futers, S.T., and Grant, P.J. (2001). Effects of novel polymorphisms in the RAGE gene on transcriptional regulation and their association with diabetic retinopathy. Diabetes *50*, 1505–1511.

Kalea, A., Schmidt, A., and Hudson, B. (2009). RAGE: a novel biological and genetic marker for vascular disease. Clin Sci *116*, 621–637.

Kalousová, M, Jáchymová, M, and Mestek, O (2007). Receptor for advanced glycation end products—soluble form and gene polymorphisms in chronic haemodialysis patients. Nephrology Dialysis Transplant 22 (7): 2020-2026.

Kang, P., Tian, C., and Jia, C. (2012). Association of RAGE gene polymorphisms with type 2 diabetes mellitus, diabetic retinopathy and diabetic nephropathy. Gene *500*, 1–9.

Kierdorf, K., and Fritz, G. (2013). RAGE regulation and signaling in inflammation and beyond. J Leukocyte Biol *94*, 55–68.

Leslie, D.R., Beyan, H., Sawtell, P., Boehm, B.O., Spector, T.D., and Snieder, H. (2003). Level of an Advanced Glycated End Product Is Genetically Determined. Diabetes *52*, 2441–2444.

Leung, C., Herath, C., Jia, Z., Andrikopoulos, S., Brown, B., Davies, M., Rivera, L., Furness, J., Forbes, J., and Angus, P. (2016). Dietary advanced glycation end-products aggravate non-alcoholic fatty liver disease. World Journal of Gastroenterology *22*, 8026.

Lorenzi, R., Grossin, N., Lambert, M., Daroux, M., Adjoutah, Z., Flahaut, C., Jacolot, P., Tessier, F., Lefranc, D., Desremaux, P., et al. (2014). Soluble form of receptor for advanced glycation end-products (sRAGE): do sRAGE ligands or anti-sRAGE auto-antibodies interfere with sRAGE quantification? Ann Clin Biochem Int J Biochem Laboratory Medicine *51*, 248–257.

Matsumoto, S, Yoshida, T, Murata, H, and Harada, S (2008). Solution structure of the variable-type domain of the receptor for advanced glycation end products: new insight into AGE− RAGE interaction†. Biochemistry.

Matsunaga-Irie, S, Maruyama, T, and Yamamoto, Y (2004). Relation Between Development of Nephropathy and the p22phox C242T and Receptor for Advanced Glycation End Product G1704T Gene Polymorphisms in Type 2 Diabetic Patients. Diabetes Care Feb 2004, 27 (2) 303-307.

Mehta, R., and Younossi, Z. (2012). Natural history of nonalcoholic fatty liver disease. Clin Liver Dis *1*, 112–113.

Mehta, R, Birerdinc, A, and Neupane, A (2013). Expression of inflammation-related genes is altered in gastric tissue of patients with advanced stages of NAFLD. Mediators of Inflammation, vol. 2013.

Metz, V., Kojro, E., Rat, D., and Postina, R. (2012). Induction of RAGE Shedding by Activation of G Protein-Coupled Receptors. Plos One *7*, e41823.

Mu, J., and Stejskalov, A. (2001). Polymorphisms 1704G/T and 2184A/G in the RAGE gene are associated with antioxidant status. Metabolism *50*, 1152–1160.

Nagendran, Moore, Norris, Khani-Hanjani, Graham, Freed, and Nagendran (2016). The varying effects of obesity and morbid obesity on outcomes following cardiac transplantation. Int J Obesity *40*, 721–724.

Neuschwander-Tetri, B. (2017). Non-alcoholic fatty liver disease. BMC Medicine *15*.

Ogden, CL, Carroll, MD, Fryar, CD, and Flegal, KM (2015). Prevalence of obesity among adults and youth: United States, 2011–2014. NCHS Data Brief.

Oliveira, M., Souza, EM, and Pedrosa, FO (2013). RAGE receptor and its soluble isoforms in diabetes mellitus complications. Jornal Brasileiro de Patologia e Medicina Laboratorial, *49*(2), 97-108.

Ott, C., Jacobs, K., Haucke, E., Santos, A., Grune, T., and Simm, A. (2014). Role of advanced glycation end products in cellular signaling. Redox Biology *2*, 411–429.

Peng, F, Hu, D, Jia, N, Li, X, Li, Y, Chu, S, Zhu, D, and Shen, W (2013). Association of four genetic polymorphisms of AGER and its circulating forms with coronary artery disease: a meta-analysis. PloS One.

Pettersson-Fernholm, K., Forsblom, C., Hudson, B.I., Perola, M., Grant, P.J., and Groop, P.-H.H. (2003). The functional -374 T/A RAGE gene polymorphism is associated with proteinuria and cardiovascular disease in type 1 diabetic patients. Diabetes *52*, 891–894.

Piperi, C., Goumenos, A., Adamopoulos, C., and Papavassiliou, A. (2015). AGE/RAGE signalling regulation by miRNAs: Associations with diabetic complications and therapeutic potential. The International Journal of Biochemistry & Cell Biology *60*, 197–201.

Preacher, K., Rucker, D., MacCallum, R., and Nicewander, A. (2005). Use of the Extreme Groups Approach: A Critical Reexamination and New Recommendations. Psychol Methods *10*, 178.

Ramasamy, Yan, and Schmidt (2009). RAGE: therapeutic target and biomarker of the inflammatory response--the evidence mounts. Journal of Leukocyte Biology *86*, 505–512.

Raucci, A., Cugusi, S., Antonelli, A., Barabino, S.M., Monti, L., Bierhaus, A., Reiss, K., Saftig, P., and Bianchi, M.E. (2008). A soluble form of the receptor for advanced glycation endproducts (RAGE) is produced by proteolytic cleavage of the membrane-bound form by the sheddase a disintegrin and metalloprotease 10 (ADAM10). FASEB J. *22*, 3716–3727.

Schaid, D. J., Rowland, C. M., Tines, D. E., Jacobson, R. M., & Poland, G. A. (2002). Score Tests for Association between Traits and Haplotypes when Linkage Phase Is Ambiguous. *American Journal of Human Genetics*, *70*(2), 425–434.

Sparvero, L.J., Asafu-Adjei, D., Kang, R., Tang, D., Amin, N., Im, J., Rutledge, R., Lin, B., Amoscato, A.A., and Zeh, H.J. (2009). RAGE (Receptor for Advanced Glycation Endproducts), RAGE ligands, and their role in cancer and inflammation. Journal of Translational Medicine *7*, 17.

Sturm, and Hattori (2012). Morbid obesity rates continue to rise rapidly in the United States. Int J Obesity *37*, 889–891.

Su, S.-C., Hsieh, M.-J., Chou, Y.-E., Fan, W.-L., Yeh, C.-B., and Yang, S.-F. (2015). Effects of RAGE Gene Polymorphisms on the Risk and Progression of Hepatocellular Carcinoma. Medicine *94*, e1396.

Takeuchi, M, Sakasai-Sakai, A, Takata, T, and Ueda, T (2015). Serum levels of toxic AGEs (TAGE) may be a promising novel biomarker in development and progression of NASH. Medical Hypotheses.

Tan, A.L., Forbes, J.M., and Cooper, M.E. (2007). AGE, RAGE, and ROS in diabetic nephropathy. *27*, 130–143.

Tomino, Y., Hagiwara, S., and Gohda, T. (2011). AGE–RAGE interaction and oxidative stress in obesity-related renal dysfunction. Kidney International *80*, 133–135.

Townsend, S.A., and Newsome, P. (2016). Non-alcoholic fatty liver disease in 2016. British Medical Bulletin *119*, 143–156.

Uribarri, J., Cai, W., Sandu, O., Peppa, M., Goldberg, T., and Vlassara, H. (2005). Diet derived advanced glycation end products are major contributors to the body's AGE pool and induce inflammation in healthy subjects. Annals of the New York Academy of Sciences *1043*, 461–466.

Uribarri, J., Woodruff, S., Goodman, S., Cai, W., Chen, X., Pyzik, R., Yong, A., Striker, G., and Vlassara, H. (2010). Advanced Glycation End Products in Foods and a Practical Guide to Their Reduction in the Diet. J Am Diet Assoc *110*, 911–916.e12.

Vazzana, N, Santilli, F, Cuccurullo, C, and Davì, G (2009). Soluble forms of RAGE in internal medicine. Internal and Emergency Medicine ed 4: 389.

Yki-Järvinen, H. (2016). Diagnosis of non-alcoholic fatty liver disease (NAFLD). Diabetologia *59*, 1104–1111.

Younossi, Reyes, Mishra, Mehta, and Henry (2014). Systematic review with meta-analysis: non-alcoholic steatohepatitis - a case for personalised treatment based on pathogenic targets. Alimentary Pharmacology & Therapeutics *39*, 3–14.

BIOGRAPHY

Gladys Shaw graduated from Saint Gertrude High School, Richmond, Virginia, in 2011. She received her Bachelor of Science from The College of William and Mary in 2015. She was employed as a graduate teaching assistant for BIOL 213: Cell Structure and Function at George Mason University, Fairfax, VA during her studies.